Hindawi
Journal of Sensors
Volume 2022, Article ID 7221294, 12 pages
https://doi.org/10.1155/2022/7221294

Research Article

Online Superficial Gas Velocity, Holdup, and Froth Depth Sensor for Flotation Cells

Claudio Leiva,[1,2] **Claudio Acuña**,[3] **Luis Bergh**,[3] **Saija Luukkanen**,[1] **and Cristóbal da Silva**[3]

[1]*Oulu Mining School, University of Oulu, 90570 Oulu, Finland*
[2]*Department of Chemical Engineering, Universidad Católica del Norte, 1270709 Antofagasta, Chile*
[3]*Department of Chemical and Environmental Engineering, Universidad Técnica Federico Santa María, 2390123 Valparaíso, Chile*

Correspondence should be addressed to Claudio Leiva; cleiva01@ucn.cl

Received 31 March 2022; Revised 4 November 2022; Accepted 29 November 2022; Published 19 December 2022

Academic Editor: Antonio Martinez-Olmos

In flotation process, the efficiency and selectivity depend on mineralogy, particle size distribution and liberation, reagents added, mixing, and particle coverage. However, the kinetics of particle recovery is highly dependent on cell hydrodynamic and circuit configuration and operational strategy. Controlling froth depth and gas flow rate, measured as superficial gas velocity, is a straightforward alternative related to kinetics in the froth and collection zones. However, these parameters are not measured accurately. Froth depth measurement is based on a floating device coupled with a sonic sensor; this configuration presents hysteresis and deviation due to variation in the gas holdup and pulp density. In self-aspirated machines, there is no technology to measure gas velocity. To address this problem, the intelligent online gas dispersion sensor based on two concentric HDPE cylindres is proposed. The intelligent online gas dispersion sensor is based on two concentric HDPE cylinders. The methodology improves the accuracy of gas velocity calculation with a new algorithm. Froth depth measurement is based on two pressure transducers, reducing the uncertainty of the floating sonic sensor to 1 cm. Pulp bulk density is directly measured, and gas holdup can be estimated. Experimental results and industrial device validation indicate that the new intelligent system can measure superficial gas velocity (Jg) online and self-calibrate, with a 2% error, the froth depth error being ±1 cm. Therefore, a multiparameter sensor for measuring gas dispersion in industrial flotation cells was experimentally designed and validated in an industrial environment (TRL 8). In this context, the proposed online gas dispersion sensor emerges as a robust technology to improve the operation of the flotation process.

1. Introduction

The flotation process is widely used to concentrate valuable mineral particles from a mixture of gangue and minerals. The concentration process collects hydrophobic particles by ascending gas bubbles [1]. This process has various interactions between elements that affect the efficiency of the process; factors such as chemical (frothers and collectors), physical (particle size and percentage of solids), type of machine, and circuit in operation are essential to overall efficiency. That is why the information collected from the multiple factors mentioned is vital in decision-making and critical to the engineering and metallurgical industry [2]. The gas bubbles collect and transport the hydrophobic mineral particles to the top of the flotation cell, forming a mineral-concentrated froth [3]. The process efficiency and kinetics depend on the hydrodynamic of particles and bubbles in the cell. It is possible to find different types of flotation machine arrangements, where there are series circuits or multiple stages [4].

In industrial flotation machines, liberation and hydrophobicity are principal parameters to control the efficiency and effectiveness of the flotation process; by adding some specific reagents called "collectors," the operator manages to selectively modify the surface properties of the mineral, making some species more hydrophobic and separating them from the other more hydrophilic species. However,

the gas flow rate and the froth depth are commonly measured and controlled to increase the concentration process efficiency [5–9]. The froth recovery influences the grade of concentrate and the overall recovery [10]. The performance of this phase is usually measured in terms of froth recovery, water recovery, and recovery of entrained minerals [11]. A clear relationship between froth stability and process performance has been shown in previous works [12]. In some plants, the discharge froth velocity is also measured by imaging systems to ensure a net mass concentrate pull; however, this strategy is not related to the metallurgical performance of the cell. The gas flow rate is measured as the total volume dispersed in the cell (average), which in large flotation units is not evenly distributed. Therefore, the rise bubble velocity cannot be determined, even though it is a key parameter to control the kinetic constant of the flotation process [13]. This parameter has multiple ways to be calculated, such as estimating the correlation between gas flow, pulp flow, and percentage of solids [14] or inserting a cylinder filled with water under the froth interface [15]. The froth depth has measured by a device that is a combination of a float and an ultrasonic sensor, which is usually uncalibrated or has a measurement bias due to froth build-up and hysteresis. The froth build-up accumulates in the floating device, changing its buoyancy, causing measurement deviations, and reducing its reliability [16, 17]. These deviations might imply 5-15% variations in recovery [18]. Given the current limitation, the flotation operation provides a stabilizing control only and, therefore, the current sensors do not contribute to controlling operation. Another method of measuring froth depth is conductivity [19]. Among the problems present are the probes used, which require constant maintenance due to direct contact with the pulp and its contamination [20].

For optimizing the flotation operation, the gas flow rate measurements require measuring gas dispersion parameters (gas holdup, surface area flux, gas velocity, froth depth, and bubble size), directly related to flotation kinetics [21]. There are different methods to measure gas velocity [22]. McGill University developed and introduced gas dispersion sensors and a hydrodynamic characterization methodology [23]. Gas dispersion analysis in flotation columns uses computational modeling [24–26].

Gas dispersion measurements in industrial flotation cells have been conducted in various cell types in the five continents by McGill University's research and development team and associated companies Cough Technologies and Nesseth. This allowed establishing the design criteria and requirements to automate the gas dispersion sensors and estimate the surface area flux and gas holdup [27, 28].

This study consists of the development, construction, implementation, and validation of an industrial prototype device for the online measurement of superficial gas velocity (Jg), pulp bulk density (RB), the volumetric fraction (Eg), and froth depth (Hf) in a flotation column. The development considers specific algorithms to automatically measure and self-calibrate gas velocity, froth depth, and pulp bulk density. Also, algorithms allow the estimation of the gas holdup, Sauter diameter, and surface area flux, the latter being a key parameter to control the kinetic process for collecting clues in the flotation machine collection zone [29].

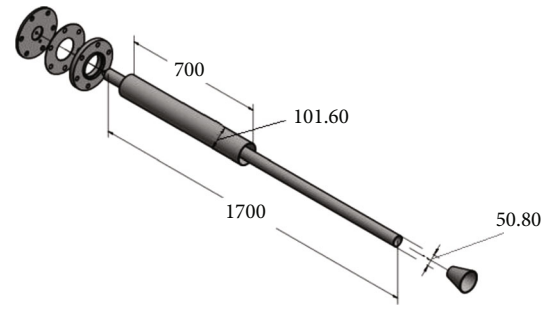

Figure 1: Double tube (mm).

The scope of this work is the industrial-scale validation of the designed sensor. Currently, the sensor has been implemented at the Las Tórtolas plant (Anglo American), and there are requests for 8 sensors for Escondida (BH Billiton) and Sierra Gorda (KGHM International).

This study is based on designing a device that allows improving the current sensors that present problems of hysteresis, out of calibrated, self-cleaning, low maintenance cost, online reading of variables that are not measured in self-aspirated cells (Jg and Eg). The developed software allows to close control loops independently or through the distributed control system of the plant. The materials and methods used for the validation and the results obtained in the three stages considered are described.

2. Materials and Methodology

The sensor uses a 50 mm–100 mm double concentric tube in the flotation cell being gas sampled. Additional to pressure measurement, there is a continuous air measurement at the tube inlet using a mass flowmeter on the top of the sampling tube. In this way, the superficial gas velocity is measured directly and continuously. It is also possible to automate the external velocity estimation (Ig), apparent density in the collection zone, gas holdup, and froth depth by using an algorithm developed.

Validation was carried out through three stages, the first was carried out at the laboratory level in a 1.2 m^3 pilot unit to ensure the correct functioning of the device. Subsequently, the sensor was installed in an industrial self-aspirated cell and validation was performed. Finally, the sensor was installed in a cell of the Tórtolas plant where it is currently operating.

2.1. Prototype Description and Design. The prototype design considers the sampling tube, a wet cabinet, and a data collection system. McGill sensor is based on the double tube and measures gas velocity by accumulation. This updated version measures the gas velocity with two concentric tubes and a mass flowmeter (calibrated by accumulation).

On the other hand, froth depth is calculated from both pressure measurements in steady state (both valves closed). The main contribution is the fully automatic McGill version. The device designed has a self-cleaning system supported by

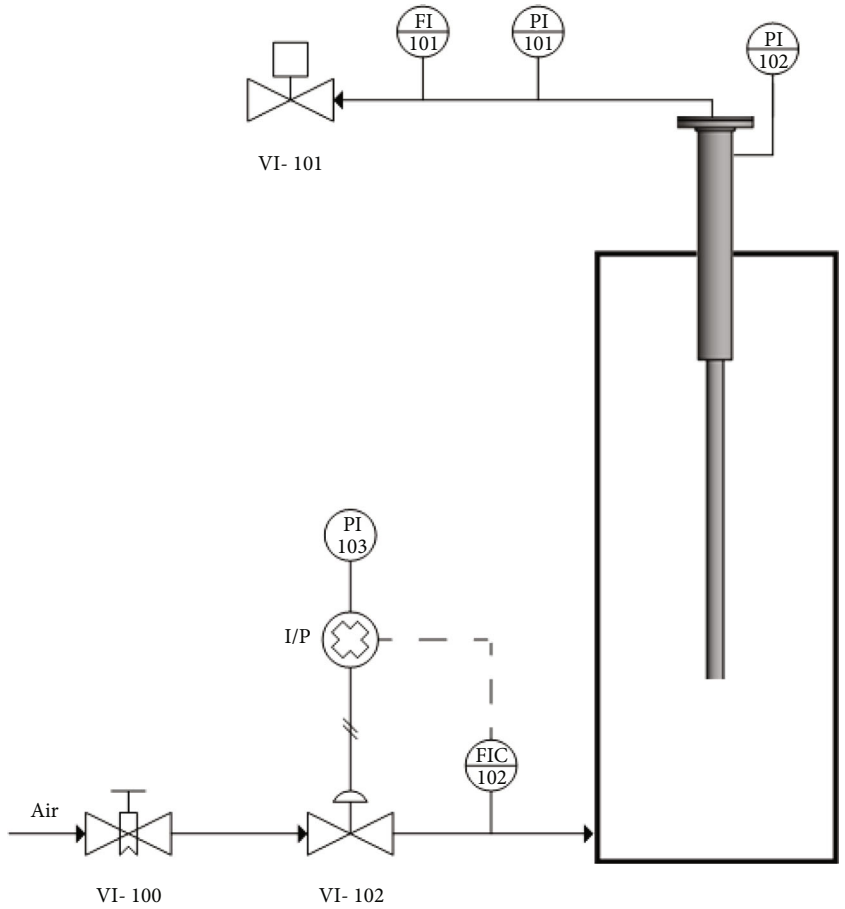

Figure 2: P&ID lab tests.

Table 1: Wet cabinet components.

Component	Specifications
Pressure sensor	Model: Wika S-20 Range: 0-4 bar Output: 4-20 mA
Solenoid valve	Model: SMC, VT307E 24 (VDC) coil
Air control valve	Model: SMC, VEX1130 Operation: 0.05–0.9 MPa Pneumatic
IP transducer	Control Air Inc. Model: type 500-AC
Flowmeter	Model: SMC, PFM7201 Range: 25 L/min and 200 L/min (SLPM) Output: 4-20 mA
Pressure regulator	Model: Foxboro Type 67 F, R28

Table 2: Data acquisition system components.

Component	Specifications
Controller	Opto 22 Snap Pac R1 12-channel rack 5 (VDC) feed
Channels	Input analog AIMA 4 (4-20 mA) Analog output SNAP AOA-23 (4-20 mA) Digital output
Sources	MW, MDR-40 series 5 V/6A and 24 V/1.7A
Computer	SLP-PPC-10AW-N2930-H-2LAN Super Logics
Screen	Super Logics SL-LCD-10WA-RTOUCH-1

air yet pulsed after each measurement. Otherwise, device has built-in a self-calibration for Jg in order to minimize errors.

2.1.1. Sampling Tube. A concentric tube design is proposed for the sampling tube to facilitate industrial installation, as

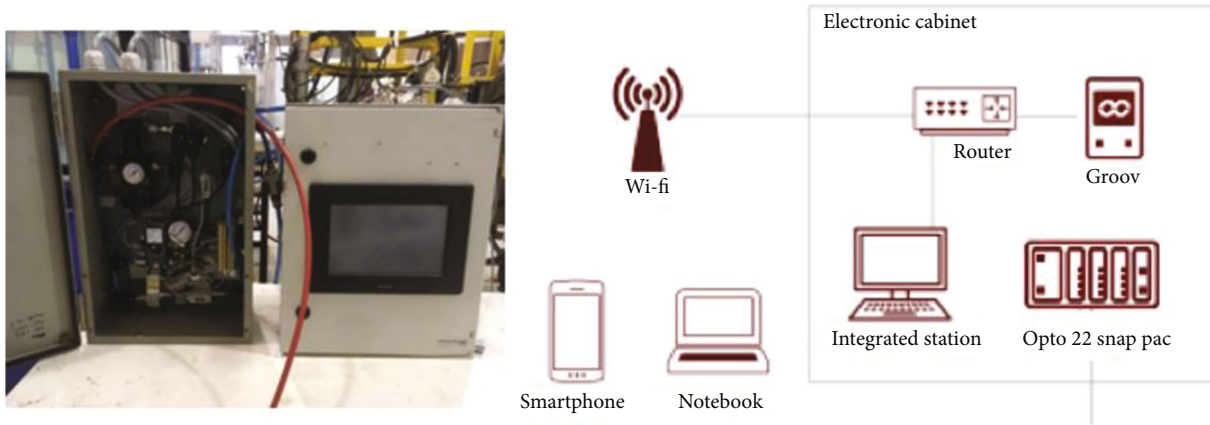

Figure 3: Opto 22 wet box (left) and touch screen hardware and connectivity diagram.

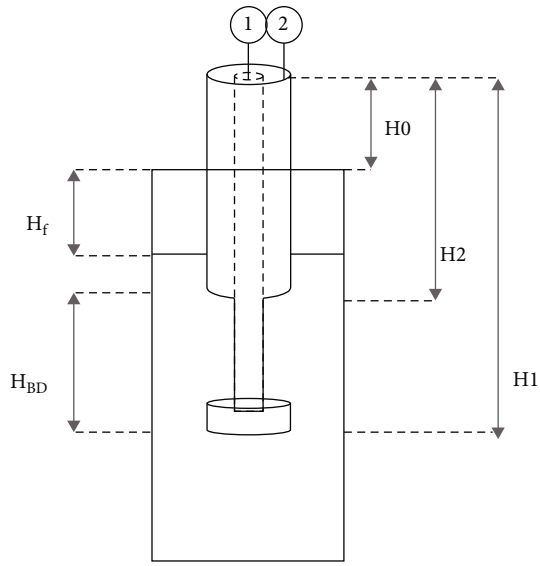

Figure 4: Double tube sensor.

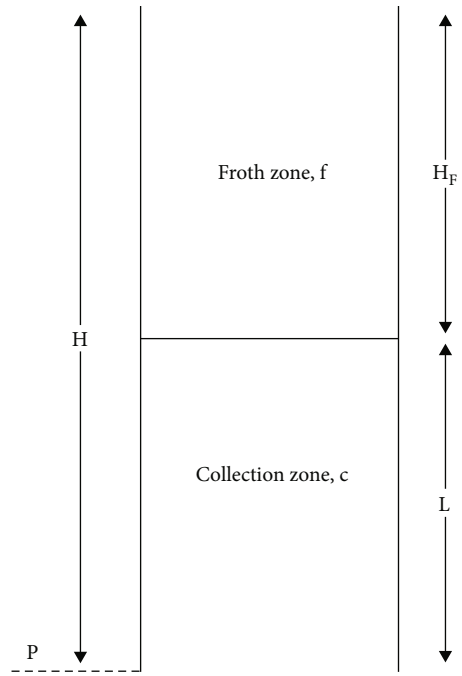

Figure 5: Hydrostatic diagram of the froth-collection interphase zone.

shown in Figure 1. The structure is put into the flotation cell and consists of pressure chambers formed of 50 mm–100 mm lines concentrically installed. These tubes are connected to the wet cabinet by two air tubings which send pressure signals to two pressure transductors and the mass airflow sensor.

A cone at the end of the inner tube increases the diameter from 50 mm to 100 mm, as shown in Figure 1. Its objective is to improve bubble capture when filling the air chamber; however, it may produce a measurement bias since its function as a channel may include, exclude, or divide the bubbles inside. Experimentally, this component tends to accelerate the air bubbles due to diameter reduction, causing the liquid to be dragged to the upper part of the tube. In practice, this device is removed because of its difficulties and has become a relevant case study for new developments not addressed in this study.

The dimensions used are based on the McGill prototype, which defines a 50 cm difference in height between the tubes [23]. The total length was experimentally defined at a lab scale. The diameters were determined via campaigns to measure the equipment developed at McGill University [23, 30]. PVC material is used in lab tests because of its manufacturing, availability, and strength feasibility.

2.1.2. Wet Cabinet: Pressure and Flow Sensors. The wet (hydraulic) cabinet holds the sensors, the receptor of the input signals coming from the concentric tube, and the output of electric signals going to the electronic cabinet, which becomes a bridge between the systems. This component is designed to improve electronics compared with the McGill prototype.

As shown in Figure 2, the wet cabinet consists of two piezoelectric pressure transducers (P101 and P102) selected for their low response time; an air mass flowmeter (F101) for Jg continuous measurement through the sampling tube;

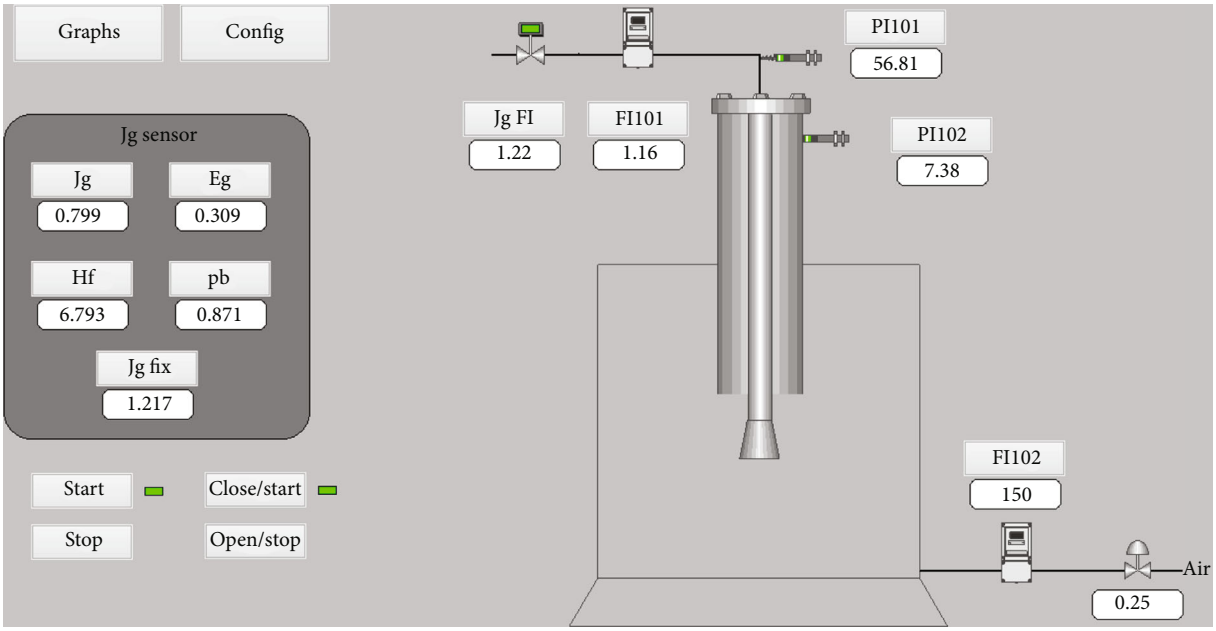

Figure 6: Sensor interface diagram.

a mass flowmeter to measure and control air injection (FIC102) in lab tests and air control regulation valve (FICV-102) and its corresponding I/P transducer with a calibration manometer (PI103); a pressure regulator (VI100) for adjusting the input air in lab tests; and a solenoid valve (VI101) to control the sensor filling cycles. Table 1 shows the technical specifications of the equipment.

2.1.3. Data Acquisition Design and Implementation. The data acquisition system (electronic cabinet) holds the central controller (16-bit resolution), an operation and registration computer, and a touch screen with HMI and data visualization. This component receives the signals from the sensors located in the hydraulic cabinet, controlling calibration and calculating the operation variables. All the details can be seen and operating with HMI by the user.

Due to the technology used, consisting of multiple input and output channels, analogue and digital, it is possible to make continuous measurements in many points of a flotation machine. Table 2 shows the data acquisition system components.

Since the original sensor measures pressures at two points in the cell, a pressure balance can be applied to determine the froth depth, which is a function of the two forces, bulk density, gas holdup, and an estimated factor for the gas holdup ratio in the collection and froth zone (i.e., 0.2).

This technology can be connected to a distributed control system. The hardware is based on Opto 22 "ultimate I /O" units to integrate the gas dispersion measurements (5 parameters) into a DCS system or local controllers, as shown in Figure 3. Groov is specific hardware to interconnect our interface with mobile devices with an industrial standard.

2.2. Jg Estimation Methodology Based on the Gas Accumulation. McGill sensor technology allows using superficial gas velocity

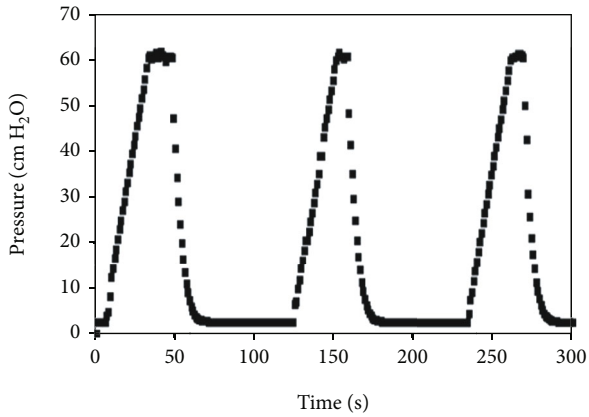

Figure 7: Dynamic pressure.

measurement techniques for applying new prototypes and redesigns. This principle is based on gas accumulation inside the pressure tubes. Using material balance and taking as a reference, the diagram is shown in Figure 4; Equation (1) can be obtained.

$$\mathrm{Jg} = \frac{P_{\mathrm{atm}} + \rho_b H_1}{\rho_b [P_{\mathrm{atm}} + \rho_b \bullet (H_1 - H_0)]} \frac{\mathrm{dp}}{\mathrm{dt}}. \quad (1)$$

Equation (1) [23] shows the pressure between the pressure accumulated in the tube and the superficial gas velocity from the hydrostatic balance. Therefore, the hydrostatic equilibrium can be used to estimate another gas dispersion parameter, i.e., the froth layer thickness.

2.3. HF Estimation from McGill Sensor. The most common method for determining froth height is pressure, that is, using a pressure sensor installed in the flotation machine.

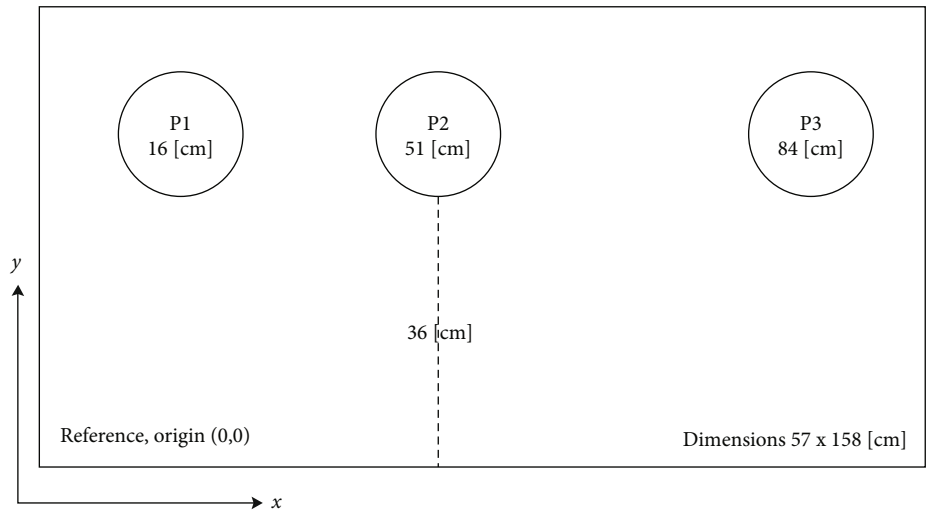

Figure 8: Upper view of lab cell measurement points.

Figure 9: Flotation cell microsphere system.

Figure 10: Microsphere flotation operation.

For this reason, by utilizing pressure sensors from the McGill prototype and under hydrostatic balance (air-filled tubes), the froth layer thickness can be estimated by using the same system that currently measures superficial gas velocity. Thus, this estimation can be analyzed, as shown in Figure 5.

Based on Figure 4, the following relationships may be determined from hydrostatics:

$$HF = \frac{H\rho_c g - p}{(\rho_b - \rho_c)g}, \tag{2}$$

where ρ_b and ρ_c are aerated pulp density and froth density, respectively, and g is gravity acceleration. The aerated pulp density can be determined by dividing the pressure difference by the tube length difference. Additionally, the froth layer density can be expressed as [30]

$$\rho_f = \rho_b\left(1 - \varepsilon_{\text{gf}}\right) + \rho_{\text{bubble}}\varepsilon_{\text{gf}}, \tag{3}$$

where ρ_b is the pulp density in the froth zone, ρ_{bubble} is the bubble density, ε_{gf} is the gas holdup in the froth zone, and ε_{gc} is the gas holdup in the collection zone. The froth layer density decomposition (Equation (3)) shows that it is difficult to determine some parameters, mainly the volumetric gas fraction and bubble density, which vary from one process to another. To simplify this equation, the term involving the product of ρ_b and ε_{gf} is neglected, since pulp density in the collection has an excellent more outstanding magnitude. In the same way, the pulp density in the collection zone can be assimilated to the pulp density in the froth zone, given the

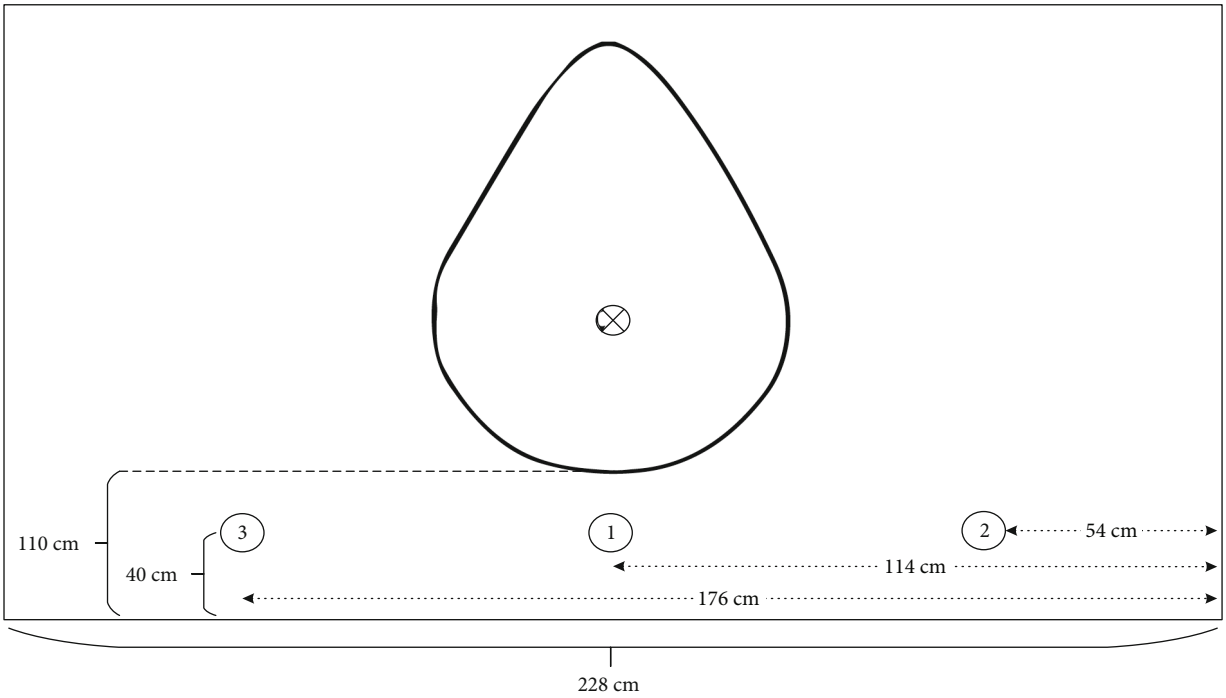

Figure 11: Upper view of sensor installation at Minera Don Alberto.

number of solids. Therefore, a heuristic relationship can be established as follows:

$$\frac{\left(1-\varepsilon_{gf}\right)}{\left(1-\varepsilon_{gc}\right)} \sim \alpha, \tag{4}$$

where in practice, parameter $\alpha = 0.2$. So, it is possible to estimate the holdup in the froth zone. In addition, this parameter can be adjusted by using calibration ε_g contrast measurement.

The holdup parameter sensitivity in the froth zone and how it affects froth height determination are analyzed. To do this, real data from one operation is used. As shown in Figure 6, the conditions are as follows: 1033 cmH_2O atmospheric pressure, 156 cm (H1) sensor length, 80 cm (H0) height from the top of the sensor to the inlet, 50 cm (Hbd) difference between tubes, P1 56.81 cmH_2O long tube pressure, P2 7.38 cmH_2O short tube pressure, 1.26 g/cm^3 pulp density, and 6.7 cm real HF froth height.

Using Equations (1)–(4), with the parameters described in the previous paragraph, the values presented in the previous figure can be obtained. Figure 7 shows the dynamic pressure behavior of the device.

According to the above, the real holdup is adjusted, and the effect of the parameter deviation on the froth layer thickness estimation is analyzed. The changes are made by ±12.5% of the delay, thus resulting in a variety of parameters α.

Since holdup is relevant for estimating the froth layer thickness, adjusting parameter α using calibration allows to obtain the corrected variable. This analysis meets a particular condition. It illustrates estimation-related problems because the parameters must be adjusted to a specific reference, considering the flotation process variability or adding a third pressure measurement point located in the froth zone [31–36].

2.4. Experimental Validation in a 1.2 m^3 Pilot Cell. Failure detection and air distribution inside an industrial flotation cell are factors that must be considered because the sensor measurement at a certain point allows locating sensors at different points to detect air distribution failures; other consideration about this validation was to implement an auto calibration system of Jg using air flowrate sensor (in industrial self-aspirated cells, this variable is not possible to measure). Then, an experiment is conducted in a 1.2 m^3 pilot cell, sampling being made in three points on two external gas flow conditions. This analysis does not consider froth layer thickness measurement due to the conditions and the lack of layer produced in the pilot cell. Considering the area available (Figure 8), it is possible to move to several cell points to obtain a gas distribution profile.

As shown in Figure 8, the point of origin (0, 0) is located at the bottom left corner of the cell. The cell dimensions are 57×118 cm. In these experiments, a floating solid was added, i.e., 0.4% p/p glass microspheres. Figures 9 and 10 show the operation with this aggregate. This solid was added to help stabilize the froth layer inside the flotation cell and generate a triphasic (solid, liquid, and gaseous) system. The frothing agent used was 9 ppm AEROFROTH 65.

The injector used for the pilot cell is a 90–250 μm microperforated hose, with 6,000 holes/m and 10 m long. The hose was mounted on acrylic support connected to the cell bottom. This configuration is expected to cover most of the equipment area and improve air distribution. The air injector moves the bubbles (swarm), which are visible at first

Figure 12: Sensor installation at Minera Don Alberto site.

Figure 13: Sensor installation at Las Tórtolas plant.

sight, toward the left part of the pilot cell and accumulates them there.

2.5. Plant Validation. The sensor was installed in the rougher circuit of the first Wemco 300 cell, in which chalcopyrite and chalcocite are principal minerals. This cell is self-aspirating and has an almost 8.5 m^3 total capacity. Figure 11 shows the cell measurement points. These allow studying the spatial distribution of the gas dispersion variables. The sensor height is changed at the three measurement points, i.e., an H0 variation is made at 90, 80, and 70 cm. In this way, the sensitivity and density effects on the aerated pulp are assessed. The superficial gas velocity is measured by analyzing its behavior and profile. In addition, the measurement of

Table 3: Experimental tests.

Test Nr.	Froth depth (cm)	Airflow rate (LPM)	Replica
1	35	5	1
2	35	10	
3	35	15	
4	25	5	
5	25	10	
6	25	15	
7	35	5	2
8	35	10	
9	35	15	
10	25	5	
11	25	10	
12	25	15	
13	35	5	3
14	35	10	
15	35	15	
16	25	5	
17	25	10	
18	25	15	

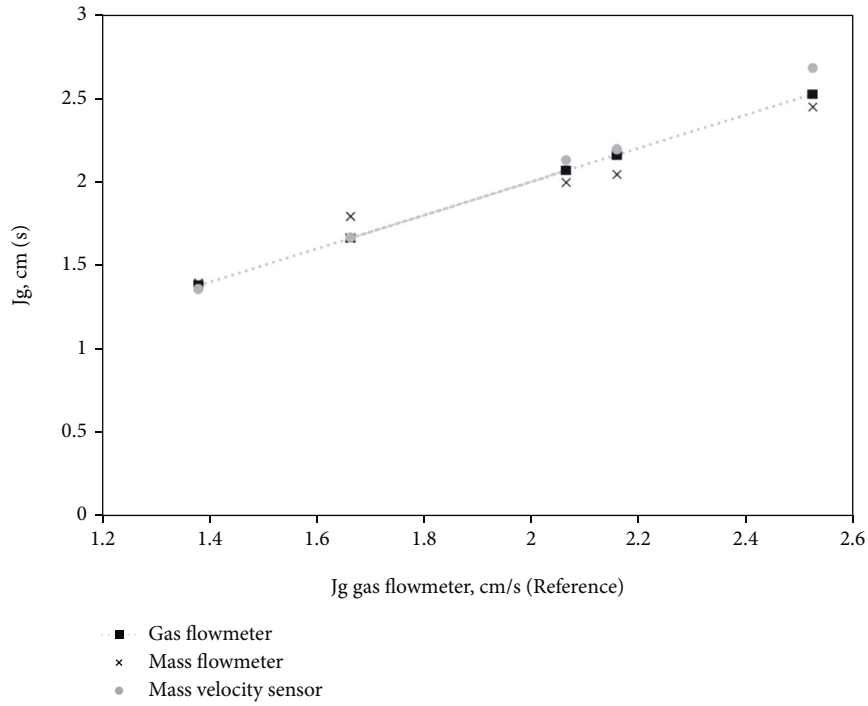

Figure 14: Gas velocity validation in pilot plant.

the froth layer thickness is evaluated by comparing the measured with afloat, which is put into the cell and hydraulically remains in the pulp-froth interphase.

During operation, the operator keeps a sample of the pulp. This parameter is measured with a Marcy direct-reading balance while feeding the conditioning tank. For calculations, the 1.26 g/cm^3 frequently measured operational density reported by the operator is considered.

The sensor is installed by fixing it with a metal beam, as shown in Figure 12. This beam is soldered to the upper part

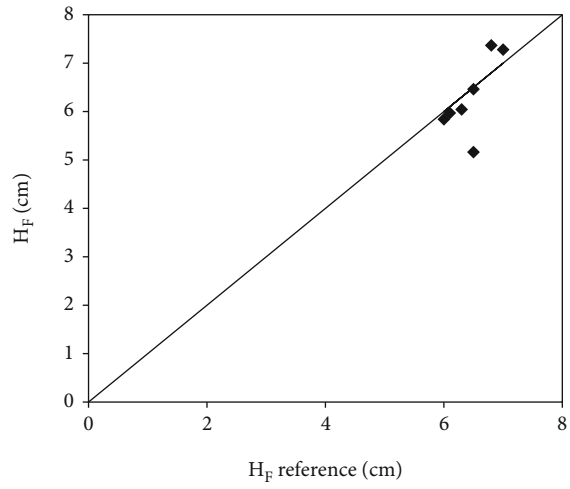

Figure 15: Froth depth validation in industrial plant.

of the cell. It has holes that let the sensor move only horizontally and vertically by using a plastic clamp that fixes it to the tube.

Figure 13 shows a real test in flotation cells in Las Tórtolas, Chile.

3. Results and Discussion

An experimental design for the different experiences is shown in Table 3, where the measurements of the gas dispersion parameters are analyzed, i.e., superficial gas velocity, froth depth, bulk density, and gas holdup. The measurements obtained with the intelligent sensor are compared with the parameters estimated theoretically. The experimental tests were conducted at two different froth depths—35 and 25 cm—and at three different airflow rates (Q)—5, 10, and 15 LPM—with 3 replicas, as shown in Table 3.

The results of the Jg validation (Figure 14) at the lab show a ±0.3 cm/s standard deviation in error, while the validation in a 1.2 m^3 cell shows a ±0.07 cm/s standard deviation in error. For in-plant validation in Wemco 300 industrial cells (12-hour shifts), froth layer, gas velocity, and pulp density measurements were made. The error in the froth layer was ±0.44 cm. Gas flow shows a parabolic profile of gas velocity (Jg) in a 0.56-1.3 cm/s range, consistent with larger-scale cells in the literature.

The validation of the system, comparing both values of Hf (calculated and measured), is shown in Figure 15.

The developed device allows online measurement of the hydrodynamic variables proposed in this study. The sensor is in the process of being patented in Chile, Peru, the USA, Australia, Canada, and Mexico. This is given the contribution to the flotation process through the online measurement of the hydrodynamic variables that allow the operator to correctly adjust (without hysteresis) the froth depth control loops and the obtaining of the parameters that allow estimating the flotation kinetics (Jg), in order to improve the grade curve and recovery of the process.

4. Conclusions and Future Work

The intelligent online gas dispersion sensor was developed based on two concentric HDPE cylinders with independently isolated pressure connectors.

The plant validation of the measurement technique based on accumulation was conducted with a reference mass flowmeter directly connected to the accumulation tube.

The validations show that the instrument can systematically and continuously infer the values of three gas dispersion, with a 15% maximum measurement error for Jg and 5% for Hf in the operating ranges (0.5-2.5 cm/s and 0-9 cm), respectively. Finally, for future work, the addition of a self-calibration system using Jg and Hf contrast with manual measurement is recommended for the commercial prototype to improve measurement robustness. Similarly, the dimensions of the sampling tubes should be studied, considering the advantages and disadvantages of error propagation in Jg and Hf estimation.

Data Availability

All raw data remains the Universidad Católica del Norte property allowed in this study. The input data used to support the endings of this study could be available from the corresponding author's email with appropriate justification.

Conflicts of Interest

The authors declare no conflict of interest.

Authors' Contributions

C.L. and C. A. conceived, designed, and performed the experiments; all the authors analyzed the data; C. L. and C.I wrote the paper.

Acknowledgments

This study received external funding from INNOVA CORFO 17-CONTEC-78906: "Desarrollo Tecnológico para la medición en línea de velocidad superficial de gas en celdas de flotación." The authors wish to acknowledge the material support provided by Minera Don Alberto and the financial support from 545-VRIDT-UCN provided by the Universidad Católica del Norte.

References

[1] R. Prakash, S. K. Majumder, and A. Singh, "Flotation technique: its mechanisms and design parameters," *Chemical Engineering and Processing-Process Intensification*, vol. 127, pp. 249–270, 2018.

[2] W. Zhang, "The effects of frothers and particles on the characteristics of pulp and froth properties in flotation—a critical review," *Journal of Minerals and Materials Characterization and Engineering*, vol. 4, no. 4, pp. 251–269, 2016.

[3] B. A. Wills and J. A. Finch, *Wills' Mineral Processing Technology: An Introduction to the Practical Aspects of Ore Treatment and Mineral Recovery*, Butterworth-Heinemann, 2015.

[4] M. Fuerstenau, G. Jameson, and R. Yoon, *Froth Flotation: A Century of Innovation*, Society for Mining, Metallurgy and Exploration Inc., Colorado, 1st edition, 2007.

[5] R. A. Grau and K. Heiskanen, "Gas dispersion measurements in a flotation cell," *Minerals Engineering*, vol. 16, no. 11, pp. 1081–1089, 2003.

[6] J. A. Torrealba-Vargas and J. A. Finch, "Continuous air rate measurement in flotation cells: some fundamental considerations," *International Journal of Mineral Processing*, vol. 81, no. 2, pp. 85–92, 2006.

[7] V. Torrealba, C. Gomez, and J. Finch, "Continuous air rate measurement in flotation cells: a step towards gas distribution management," *Minerals Engineering*, vol. 17, no. 6, pp. 761–765, 2004.

[8] J. Nesset and F. Cappuccitti, *Frother and collector effects on flotation cell hydrodynamics and their implication on circuit performance*, Canadian Institute of Mining, Metallurgy and Petroleum., 2006.

[9] F. Seguel, I. Soto, N. Krommenacker, M. Maldonado, and N. B. Yoma, "Optimizing flotation bank performance through froth depth profiling: revisited," *Minerals Engineering*, vol. 77, pp. 179–184, 2015.

[10] M. Reza, A. Seher, and J. Graeme, "Study of froth behaviour in a controlled plant environment - Part 1: effect of air flow rate and froth depth," *Minerals Engineering*, vol. 81, pp. 152–160, 2015.

[11] B. Comley, M. Vera, and J.-P. Franzidis, "Interpretation of the effect of frother type and concentration on flotation performance in an OK3 cell," *Minerals & Metallurgical Processing*, vol. 24, no. 4, pp. 243–252, 2007.

[12] K. Hadler, N. Plint, J. Cilliers, and M. Greyling, "The effect of froth depth on air recovery and flotation performance," *Minerals Engineering*, vol. 36-38, pp. 248–253, 2012.

[13] G. Dobby, J. Yianatos, and J. Finch, "Estimation of bubble diameter in flotation columns from drift flux analysis," *Canadian Metallurgical Quarterly*, vol. 27, no. 2, pp. 85–90, 1988.

[14] M. Falutsu, "Direct measurement of gas rate in a flotation machine," *Minerals Engineering*, vol. 7, no. 12, pp. 1487–1494, 1994.

[15] G. Jameson and P. Allum, *A survey of bubbles sizes in industrial flotation cells*, Report prepared for AMIRA limited, 1984.

[16] L. Bergh and J. Yianatos, "Flotation column automation: state of the art," *Control Engineering Practice*, vol. 11, no. 1, pp. 67–72, 2003.

[17] R. Rule, *Flotation Level Measurement Techniques*, Creamer Media's Eng. News, 2017, http://www.engineeringnews.co.za/article/flotation-level-measurement-techniques-2017-03-31/rep_id:4136.

[18] R. M. Rahman, S. Ata, and G. J. Jameson, "Study of froth behaviour in a controlled plant environment - part 1: effect of air flow rate and froth depth," *Minerals Engineering*, vol. 81, pp. 152–160, 2015.

[19] M. Maldonado, A. Desbiens, and R. del Villar, "An update on the estimation of the froth depth using conductivity measurements," *Minerals Engineering*, vol. 21, no. 12–14, pp. 856–860, 2008.

[20] L. Bergh and J. Yianatos, "Control alternatives for flotation columns," *Minerals Engineering*, vol. 6, no. 6, pp. 631–642, 1993.

[21] M. Cooper, D. Scott, R. Dahlke, J. A. Finch, and C. O. Gomez, "Impact of air distribution profile on banks in a Zn cleaning circuit," *CIM Bulletin*, vol. 97, no. 1083, pp. 1–6, 2004.

[22] J. Yianatos, L. Bergh, P. Condori, and J. Aguilera, "Hydrodynamic and metallurgical characterization of industrial flotation banks for control purposes," *Minerals Engineering*, vol. 14, no. 9, pp. 1033–1046, 2001.

[23] C. Gomez and J. Finch, "Gas dispersion measurements in flotation cells," *Mineral Processing*, vol. 84, no. 1-4, pp. 51–58, 2007.

[24] I. Mwandawande, *Investigation of the Gas Dispersion and Mixing Characteristics in Column Flotation Using Computational Fluid Dynamics (CFD) (Extractive Metallurgical Engineering)*, Doctoral dissertation, Stellenbosch: Stellenbosch University, 2016.

[25] I. Mwandawande, G. Akdogan, S. M. Bradshaw, M. Karimi, and N. Snyders, "Prediction of gas holdup in a column flotation cell using computational fluid dynamics (CFD)," *Journal of the Southern African Institute of Mining and Metallurgy*, vol. 119, no. 1, pp. 81–95, 2019.

[26] P. T. L. Koh, M. P. Schwarz, Y. Zhu, P. Bourke, R. Peaker, and J. P. Franzidis, "Development of CFD models of mineral flotation cells," in *Third International Conference on Computational Fluid Dynamics in the Minerals and Process Industries*, Melbourne, Australia, 2003.

[27] J. E. Nesset, J. Hernandez-Aguilar, C. Acuna, C. Gomez, and J. Finch, "Some gas dispersion characteristics of mechanical flotation machines," *Minerals Engineering*, vol. 19, no. 6-8, pp. 807–815, 2006.

[28] E. Matiolo, F. Testa, J. Yianatos, and J. Rubio, "On the gas dispersion measurements in the collection zone of flotation columns," *International Journal of Mineral Processing*, vol. 99, no. 1-4, pp. 78–83, 2011.

[29] B. Gorain, J. Franzidis, and E. Manlapig, "Studies on impeller type, impeller speed and air flow rate in an industrial scale flotation cell. Part 4: effect of bubble surface area flux on flotation performance," *Minerals Engineering*, vol. 10, no. 4, pp. 367–379, 1997.

[30] R. Araya, *Gas distribution in industrial flotation machines: a proposed measurement method*, McGill University, 2009.

[31] J. Finch and G. Dobby, *Column Flotation*, Pergamon Press, 1st edition, 1991.

[32] M. Ostadrahimi, S. Farrokhpay, K. Gharibi, A. Dehghani, and M. Aghajanloo, "Effects of flotation operational parameters on froth stability and froth recovery," *Journal of the Southern African Institute of Mining and Metallurgy*, vol. 121, no. 1, pp. 11–20, 2021.

[33] F. Nakhaei, M. Irannajad, and S. Mohammadnejad, "A comprehensive review of froth surface monitoring as an aid for grade and recovery prediction of flotation process. Part B: texture and dynamic features," *Energy Sources, Part A: Recovery, Utilization, and Environmental Effects*, pp. 1–23, 2019.

[34] F. Nakhaei, M. Irannajad, and S. Mohammadnejad, "Evaluation of column flotation froth behavior by image analysis: effects of operational factors in desulfurization of iron ore concentrate," *Energy Sources, Part A: Recovery, Utilization, and Environmental Effects*, vol. 40, no. 19, pp. 2286–2306, 2018.

[35] B. McFadzean, T. Marozva, and J. Wiese, "Flotation frother mixtures: decoupling the sub-processes of froth stability, froth recovery and entrainment," *Minerals Engineering*, vol. 85, pp. 72–79, 2016.

[36] I. Ramos, M. Maldonado, D. Meriño, P. Bustos, F. Henriquez, and M. Morales, "A new approach to measure gas holdup in industrial flotation machines. Part III: industrial prototype design and assessment," *Minerals Engineering*, vol. 180, article 107490, 2022.